# A structure and magnetic properties of one-dimensional manganese/cobalt coordination polymers with 5-nitro-1,3-benzenedicarboxylic acid and imidazole

Hong-Ji Chen[a]; Yan-Guo Li[a]

[a] Department of Material Science and Engineering, Jinan University, Guangzhou 510632, P.R. China

Online publication date: 22 September 2010

## PLEASE SCROLL DOWN FOR ARTICLE

Taylor & Francis
Taylor & Francis Group

# A structure and magnetic properties of one-dimensional manganese/cobalt coordination polymers with 5-nitro-1,3-benzenedicarboxylic acid and imidazole

HONG-JI CHEN* and YAN-GUO LI

Department of Material Science and Engineering, Jinan University,
Guangzhou 510632, P.R. China

One-dimensional manganese(II) complex, $[Mn_2(5\text{-}nbdc)_2(imH)_6] \cdot 2H_2O$ (**1**) (5-nbdcH$_2$ = 5-nitro-1,3-benzenedicarboxylic acid and imH = imidazole), has been hydrothermally synthesized and structurally characterized by X-ray crystallography with the following data: orthorhombic, space group $Pna2(1)$, $M_r = 972.63$ for $Mn_2C_{34}H_{34}N_{14}O_{14}$, $a = 13.3391(12)$ Å, $b = 16.4657(15)$ Å, $c = 18.2177(16)$ Å; $V = 4001.3(6)$ Å$^3$, $Z = 4$, $D_{calcd}$ 1.615 g cm$^{-3}$, $\mu = 0.718$ mm$^{-1}$, the final $R = 0.0490$ and $wR = 0.1277$ for 7278 observed reflections $(I > 2\sigma(I))$. Complex **1** exhibits very weak intra-chain ferromagnetic coupling $(J\,k^{-1} = 0.001\,K)$ with g = 1.930. The magnetism of a one-dimensional cobalt(II) complex $[Co(5\text{-}nbdc)_2(imH)_2]_n$ (**2**) indicates weak intra-chain anti-ferromagnetic coupling $(J\,k^{-1} = -0.067\,K)$ with $g = 2.0791$.

*Keywords*: Coordination polymer; Manganese; Cobalt, Magnetic property; Crystal structure

## 1. Introduction

The design and synthesis of coordination polymers is a developing field in both chemistry and material science due to structural diversity and physical properties such as gas adsorption [1–3], photoluminescence [4, 5], non-linear optics [6] and light-weight molecular-based magnets [7–9]. Magnetic systems extending along one-dimension, with linear magnetic response, are excellent examples to develop models for better understanding of exchange interactions in extended structures. In order to build a well-defined framework, bridging ligands play an important role in connecting paramagnetic metal centers, mediating super-exchange interactions, and supporting the molecular arrangement in a crystal. 5-nitro-1,3-benzenedicarboxylate is an excellent bridging ligand, which has been efficiently used for creating solid-state architecture with transition metal ions through its versatile binding modes and flexible conformation as well as through specific and directional hydrogen bonds increasing the molecular dimensionality [10, 11]. Here we report two one-dimensional coordination polymers, $[Mn_2(5\text{-}nbdc)_2(imH)_6] \cdot 2H_2O$ (**1**)

---

*Corresponding author. Email: thjchen@jnu.edu.cn

and $[Co(5\text{-}nbdc)_2(imH)_2]_n$ (**2**) (5-nbdcH$_2$ = 5-nitro-1,3-benzenedicarboxylic acid and imH = imidazole), and investigate their magnetic properties.

## 2. Experimental

### 2.1. *Preparation*

Synthesis of $[Mn_2(5\text{-}nbdc)_2(imH)_6] \cdot 2H_2O$ (**1**). Complex **1** was obtained by hydrothermal reaction from a mixture of manganese chloride tetrahydrate, 5-nitro-1,3-benzenedicarboxylic acid, imidazole and water in a polyfluoroethylene lined stainless steel bomb (25 mL capacity) under autogenous pressure. Yellow crystals were grown at 433 K for three days in 55% yield. A mixture containing manganese chloride tetrahydrate (0.198 g, 1.0 mmol), 5-nitro-1,3-benzenedicarboxylic acid (0.211 g, 1.0 mmol), imidazole (0.2044 g, 3.0 mmol) and 10 mL of water in a 25 mL Teflon container was stirred and then heated at 150°C for four days. After decreasing to room temperature slowly, yellow crystals suitable for X-ray analysis were obtained. IR data (cm$^{-1}$): 3213(s), 1619(vs), 1537(s), 1453(m), 1428(s), 1370(vs), 1326(m), 1255(w), 1098(w), 1066(vs), 789(m), 729(s), 657(s). Elemental analysis, found: C, 33.78; H, 1.99; N, 10.92; O, 29.02. Calcd for Mn$_2$C$_{34}$H$_{34}$N$_{14}$O$_{14}$: C, 33.92; H, 2.07; N, 10.79; O, 28.75.

Synthesis of $[Co(5\text{-}nbdc)_2(imH)_2]_n$ (**2**). Complex **2** was prepared according to our reported method [17].

### 2.2. *X-ray single crystal structure determination*

Crystallographic analysis for Mn$_2$C$_{34}$H$_{34}$N$_{14}$O$_{14}$: $F_w = 972.63$, $T = 173(2)$ K, Orthorhombic, space group *Pna*2(1), $a = 13.3391(12)$ Å, $b = 16.4657(15)$ Å, $c = 18.2177(16)$ Å; $V = 4001.3(6)$ Å$^3$, $Z = 4$, crystal color yellow, crystal size $0.48 \times 0.33 \times 0.22$ mm$^3$, $D_{calcd}$ 1.615 g cm$^{-3}$, $R_1 = 0.0490$, $wR_2 = 0.1277$, $2.26 < \theta < 26.98°$, reflections collected 22961, data/restraints/parameters 7278/7/577, residual maximum and minimum in the final Fourier difference maps were 0.8580 and 0.7244 Å$^{-3}$. Diffraction data were collected on a Bruker Smart 1000 CCD diffractometer using an $\omega$–$2\theta$ scan mode. The data were corrected with SADABS programs and refined on $F^2$ with SHELXL software [12]. The structure was solved by direct methods and refined by using full-matrix least-squares difference Fourier techniques with the SHELXS-97 and SHELXL-97 program packages [12, 13]. All non-hydrogen atoms were refined with anisotropic displacement parameters. All hydrogen atoms of the ligand were placed at idealized positions and refined as riding atoms with the relative isotropic parameters of the heavy atoms to which they are attached. The drawings were produced with SHELXTL [14]. CCDC reference numbers: 646193 for **1**.

## 3. Results and discussion

In the infrared spectra of **1**, the $\nu_{N-H}$ characteristic vibrations for terminal coordinate imidazole molecules are at 3213 cm$^{-1}$. One strong $\nu_{as}(COO^-)$ characteristic band at

$1619 \, \text{cm}^{-1}$ and two other strong $\nu_s(\text{COO}^-)$ bands at $1428 \, \text{cm}^{-1}$ and $1370 \, \text{cm}^{-1}$, respectively, confirm that the tridentate bridging ligand, $\mu$-O$_3$-5-nitro-1,3-benzenedicarboxylate, exists in **1** ($\Delta \nu = \nu_{as}(\text{COO}^-) - \nu_s(\text{COO}^-) = 191$ and $249 \, \text{cm}^{-1}$) [15, 16]. Two medium-intensity bands at $1537 \, \text{cm}^{-1}$ and $1345 \, \text{cm}^{-1}$ are assigned to the asymmetric and symmetric stretching frequencies of NO$_2$ group on the phenyl.

The X-ray diffraction analysis indicates that **1** is neutral polymeric chains [Mn$_2$(5-nbdc)$_2$(imH)$_6$]$_n$ and lattice water molecules. The coordination environment around Mn(II) with atom-numbering scheme is depicted in figure 1. There are two independent Mn(II) centers (Mn1 and Mn2) in the repeat unit of **1**. Three oxygen donors from two 5-nitro-1,3-benzenedicarboxylic acid ligands and three nitrogen donors from imidazole molecules define the distorted octahedral coordination environment of Mn(II). Three oxygen atoms from two different $\mu$-O$_3$-5-nitro-1,3-benzenedicarboxylates and a nitrogen from a coordinated imidazole are in the equatorial positions and two nitrogens from coordinated imidazoles occupy axial sites. For Mn1, the axial Mn–N bond distances [2.221(3) and 2.224(4) Å] are significantly longer than the equatorial Mn–N bond distance [2.186(4) Å]; the equatorial Mn–O bond distance [2.150(3) Å] from the monodentate $\mu$-O$_3$-5-nitro-1,3-benzenedicarboxylate group is significantly shorter than that [2.330(3) and 2.375(3) Å] from the bidentate $\mu$-O$_3$-5-nitro-1,3-benzenedicarboxylate group. The bond angles around Mn1 change from 56.13(11) to 97.48(12)°. Similar to Mn1, Mn2 shows longer axial Mn–N bond distances [2.227(3) and 2.230(3) Å] than equatorial and the equatorial Mn2–O bond distance [2.118(3) Å] for the monodentate group is somewhat shorter than that [2.227(3) and 2.488(3) Å] from the bidentate one. Both Mn1 and Mn2 exhibit similar coordination environments but different bond parameters. Mn1 and Mn2 are bonded to six nitrogens of imidazole and bridged by an $\mu$-O$_3$-5-nitro-1,3-benzenedicarboxylate group forming a dimer Mn$_2$(5-nbdc)(imH)$_6$ with a Mn1–Mn2 distance of 8.752 Å;
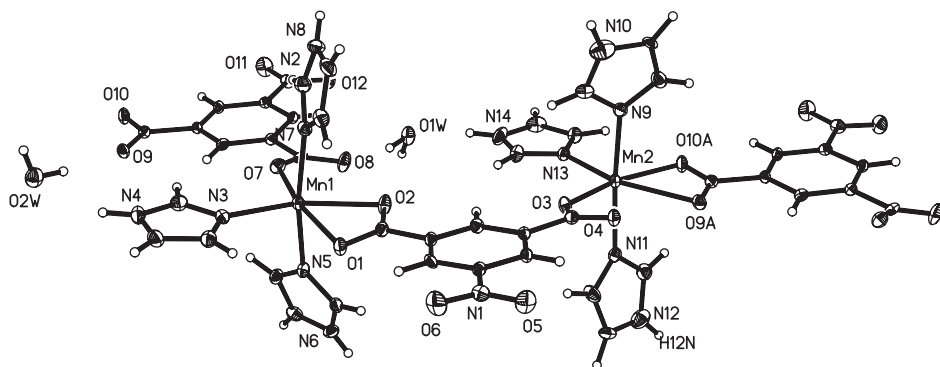


Figure 1. Perspective view of the one-dimensional chain of **1**. Selected bond lengths (Å) and angles (°): Mn1–O1 2.375(3), Mn1–O2 2.330(3), Mn1–O7 2.150(3), Mn1–N3 2.186(4), Mn1–N5 2.224(4), Mn1–N7 2.221(3), Mn2–O3 2.118(3), Mn2–O9a 2.488(3), Mn2–O10a 2.227(3), Mn2–N9 2.230(3), Mn2–N11 2.227(3), Mn2–N13 2.182(4), O7–Mn1–N3 99.11(14), O7–Mn1–N7 88.51(12), N3–Mn1–N7 92.85(12), O7–Mn1–N5 86.94(12), N3–Mn1–N5 97.48(12), N7–Mn1–N5 169.26(14), O7–Mn1–O2 111.69(12), N3–Mn1–O2 148.82(13), N7–Mn1–O2 83.54(11), N5–Mn1–O2 89.11(11), O7–Mn1–O1 167.32(12), N3–Mn1–O1 93.36(13), N7–Mn1–O1 93.18(12), N5–Mn1–O1 89.19(11), O2–Mn1–O1 56.13(11), O3–Mn2–N13 99.22(14), O3–Mn2–O10a 161.96(12), N13–Mn2–O10a 98.80(13), O3–Mn2–N11 88.32(12), N13–Mn2–N11 94.91(12), O10a–Mn2–N11 91.02(12), O3–Mn2–N9 87.57(12), N13–Mn2–N9 93.73(12), O10a–Mn2–N9 90.39(12), N11–Mn2–N9 170.92(14), O3–Mn2–O9a 106.25(11), N13–Mn2–O9a 154.47(13), O10a–Mn2–O9a 55.77(11), N11–Mn2–O9a 84.30(10), N9–Mn2–O9a 89.09(10) (symmetry code: *a*, *x*, *y* + 1, *z*).

adjacent dimers are further linked by $\mu$-$O_3$-5-nitro-1,3-benzenedicarboxylate groups generating the neutral polymeric chain $[Mn_2(5\text{-nbdc})_2(imH)_6]$ with a Mn2–Mn1a separation of 8.991 Å, showing a *syn–anti* geometry. Finally, adjacent chains are further linked by weak hydrogen bonds (hydrogen bond N6–H$\cdots$O4i = 2.843(4), N8–H$\cdots$O9ii = 2.918(5) Å; symmetry code: i, $x+1/2$, $-y+3/2$, $z$; ii, $x-1/2$, $-y+1/2$, $z$) extending into an infinite two-dimensional network with Mn–Mn separation of 8.106 Å (figure 2).

The X-ray crystal structure analysis shows that $[Co(5\text{-nbdc})_2(imH)_2]_n$ (**2**) is a one-dimensional neutral chain with *syn–syn* geometry [17]. Adjacent cobalt(II) atoms with the same coordination environment lay along a straight line with a Co–Co separation of 9.525 Å.

The magnetic susceptibilities ($\chi_M$) were measured at 10 kOe in the variable-temperature range 2–300 K and the $\chi_M$ and $\chi_M T$ *versus* $T$ plots for **1** are given in figure 3. The $\chi_M$ value increases slowly in the temperature range 300–50 K and increases quickly up to 3.20 cm$^3\cdot$mol$^{-1}$ at 2.0 K. The $\chi_m T$ product at room temperature is 4.40 cm$^3$ mol$^{-1}$ K, in agreement with that expected for spin-only (4.38 cm$^3$ mol$^{-1}$ K) of one magnetically uncoupled manganese(II) [18]. Upon cooling, the $\chi_m T$ value decreases slowly in the temperature range 300–20 K. In the temperature range 20–15 K there is an approximate plateau with $\chi_m T = 4.06$ cm$^3$ mol$^{-1}$ K. Below 15 K, the $\chi_m T$ value decreases slowly to 3.98 cm$^3$ mol$^{-1}$ K as the zero field splitting (ZFS) of the ground state of the manganese(II). The overall magnetic behavior of the complex suggests very weak ferromagnetic interaction between the spin carriers and resembles that of related infinite chain model compounds [19].

The X-ray crystal structure analysis of **1** shows that the polymeric chain is composed of a Mn1–Mn2 dimer linked by $\mu$-$O_3$-5-nitro-1,3-benzenedicarboxylate bridges with Mn–Mn separations of 8.752 and 8.991 Å. In order to simplify the calculation, the spin
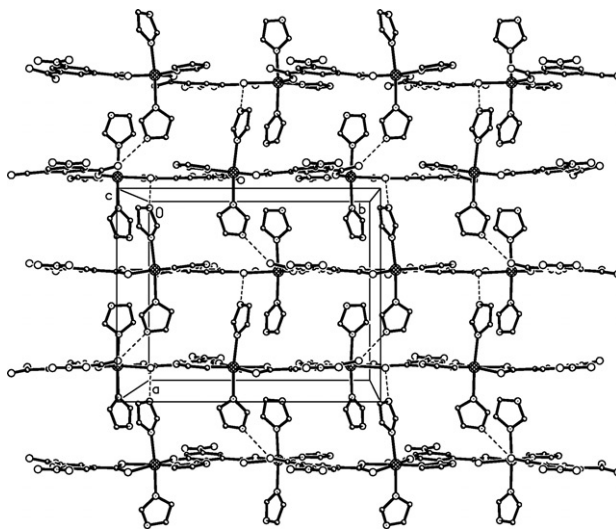


Figure 2. Perspective view of the two-dimensional hydrogen bond network of **1** running along the *ab* plane. Hydrogen atoms and lattice water molecules are omitted for clarity. Hydrogen bond N6–H$\cdots$O4i = 2.843(4), N8–H$\cdots$O9ii = 2.918(5) Å. Symmetry code: i, $x+1/2$, $-y+3/2$, $z$; ii, $x-1/2$, $-y+1/2$, $z$.

Hamiltonian appropriate for describing the linear chain is given in equation (1). The magnetic susceptibility deduced from the Hamiltonian for local spin values $S = 5/2$ is as in equation (2), where $J$ denotes the exchange parameter between adjacent manganese atoms in the chain [20, 21].

$$H = -J\Sigma S_i S_{i+1} \tag{1}$$

$$\chi_{\text{chain}} = \frac{Ng^2\mu_B^2}{k_B T} \times \frac{2.9167 + 208.04x^2}{1 + 15.453x + 2707.2x^3}.$$
$$\left( x = \frac{J}{kT} \right) \tag{2}$$

The magnetic data of **1** were analyzed by means of the analytical expression based on the Hamiltonian (1) for local spin values $S = 5/2$ [22, 23]. The experimental data were fitted by least-squares and the resulting parameters are $J/k = 0.001\,\text{K}$, $g = 1.93$ and $R = 3.03 \times 10^{-6}$ $(R = \Sigma[(\chi_m)_{\text{obs}} - (\chi_m)_{\text{calcd}}]^2 / \Sigma[(\chi_m)_{\text{obs}}]^2)$. The small $J$ value suggests almost no ferromagnetic coupling along the chain in the coordination polymer [23].

The temperature dependence of $\chi_M T$ product measured at $10\,\text{kOe}$ for **2** in the variable-temperature range $2$–$300\,\text{K}$ is shown in figure 4. The overall magnetic behavior of the complex is dominated by anti-ferromagnetic interaction between the spin carriers and resembles that of related infinite chain model compounds [24–26]. The $\chi_m T$ product at room temperature is about $2.18\,\text{cm}^3\,\text{mol}^{-1}\,\text{K}$, somewhat higher

Figure 3. Temperature dependence of $\chi_M T$ for **1** measured at $10\,\text{kOe}$. The solid line corresponds to the best theoretical fit for the data in the $2$–$300\,\text{K}$ range.
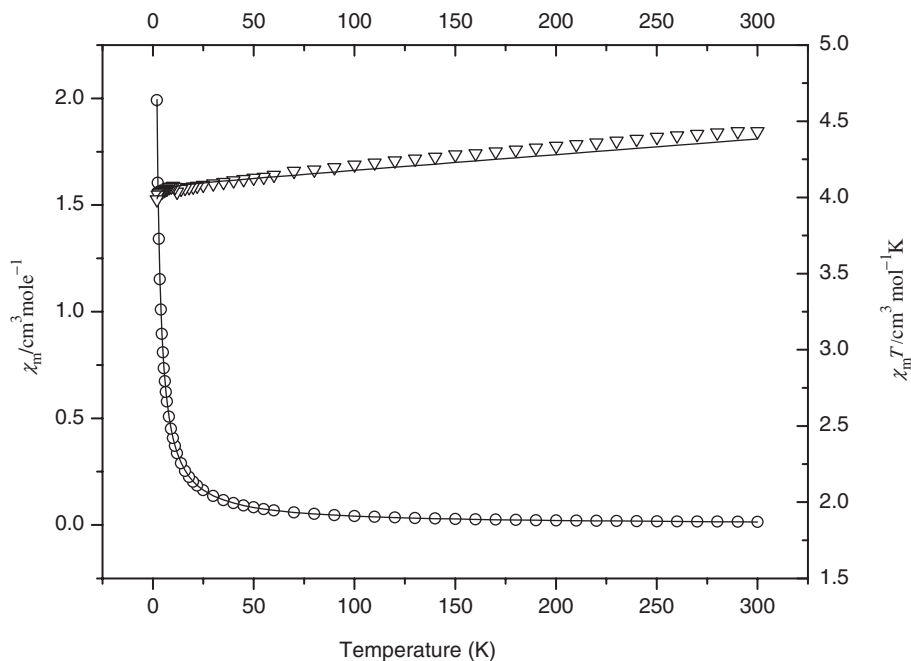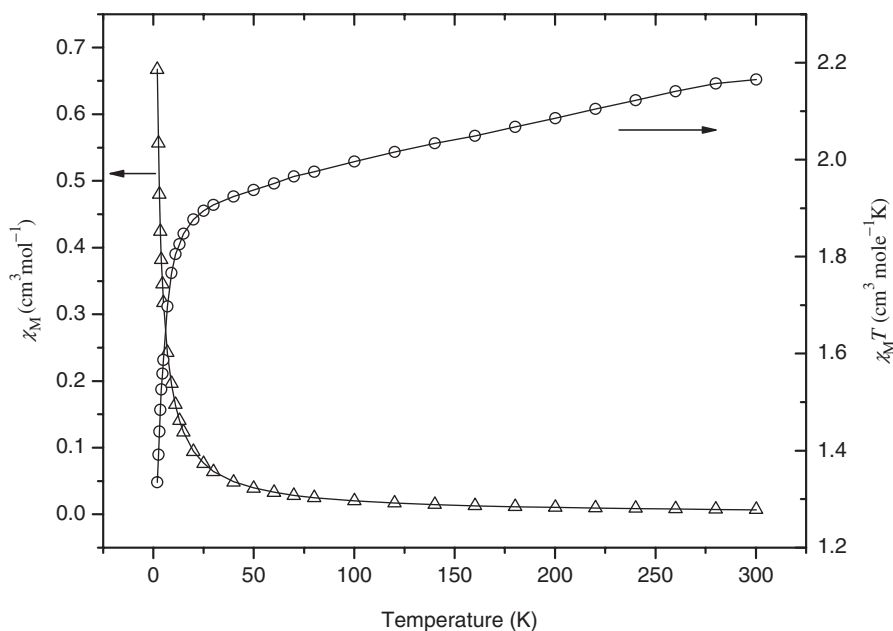
Figure 4. Temperature dependence of $\chi_M T$ for **2** measured at 10 kOe. The solid line corresponds to the best theoretical fit for the data in the 2–300 K range.

than that expected for one magnetically uncoupled cobalt ion ($1.95\,\text{cm}^3\,\text{mol}^{-1}\,\text{K}$). Upon cooling, the $\chi_m T$ value decreases slowly in the temperature range 300–25 K from the anti-ferromagnetic interaction between the cobalt(II) ions within the chain. Below 25 K the $\chi_m T$ value decreases quickly down to $1.30\,\text{cm}^3\,\text{mol}^{-1}\,\text{K}$ as the zero field splitting of the ground state of cobalt(II).

In **2**, adjacent cobalt(II) atoms with the same coordination environment lay along a straight line with a Co–Co separation of 9.525 Å, similar to that of a cobalt(II) chain [25]. The magnetic susceptibility deduced from the Hamiltonian for local spin values $S = 3/2$ is given in equation (3).

$$\chi_{\text{chain}} = \frac{Ng^2\mu_B^2}{k_B T} \times \frac{1.2500 + 17.041x^2}{1 + 6.7360x + 238.47x^3}.$$

$$x = \frac{|J|}{k_B T}$$

(3)

The overall magnetic behavior of **2** corresponds to an anti-ferromagnetic coupled system. The magnetic data of **2** were analyzed by means of the analytical expression (1) for the magnetic susceptibility of an infinite chain with local spin values $S = 3/2$. The experimental data were fitted by least-squares and the resulting parameters are $J/k = -0.067\,\text{K}$, $g = 2.0791$ and $R = 1.00 \times 10^{-5}$ ($R = \Sigma[(\chi_m)_{\text{obs}} - (\chi_m)_{\text{calcd}}]^2 / \Sigma[(\chi_m)_{\text{obs}}]^2$). The small $J$ value suggests that **2** shows very weak anti-ferromagnetic coupling along the chain in the coordination polymer.

## Acknowledgements

## References

[1] S. Kitagawa, R. Kitaura, S.-I. Noro. *Angew. Chem. Int. Ed.*, **43**, 2334 (2004).
[2] J.L.C. Rowsell, J. Eckert, O.M. Yaghi. *J. Am. Chem. Soc.*, **127**, 14904 (2005).
[3] W. Chen, H.-M. Yuan, J.-Y. Wang, Z.-Y. Liu, J.-J. Xu, M. Yang, J.-S. Chen. *J. Am. Chem. Soc.*, **125**, 9266 (2003).
[4] C. Janiak. *Dalton Trans.*, 2781 (2003).
[5] J.-P. Zhang, Y.-Y. Lin, X.-C. Huang, X.-M. Chen. *J. Am. Chem. Soc.*, **127**, 5495 (2005).
[6] W. Lin, M.E. Chapman, Z.Y. Wang, G.T. Yee. *Inorg. Chem.*, **39**, 4169 (2000).
[7] S. Mandal, M.A. Green, S. Natarajan, S.K. Pati. *J. Phys. Chem. B*, **108**, 20351 (2004).
[8] X.-Y. Wang, H.-Y. Wei, Z.-M. Wang, Z.-D. Chen, S. Gao. *Inorg. Chem.*, **44**, 572 (2005).
[9] S. Hill, R.S. Edwards, N. Aliaga-Alcalde, G. Christou. *Science*, **302**, 1015 (2003).
[10] J.-H. Luo, M.-C. Hong, R.-H. Wang, R. Cao, L. Han, Z.-Z. Lin. *Eur. J. Inorg. Chem.*, 2705 (2003).
[11] J.-H. Luo, M.-C. Hong, R.-H. Wang, R. Cao, L. Han, D.-Q. Yuan, Z.-Z. Lin, Y.-F. Zhou. *Inorg. Chem.*, **42**, 4486 (2003).
[12] G.M. Sheldrick. *SHELXS-97, Program for X-ray Crystal Structure Determination*, Göttingen University, Germany (1997).
[13] G.M. Sheldrick. SHELXL-97, *Program for X-ray Crystal Structure Refinement*, Göttingen University, Germany (1997).
[14] G.M. Sheldrick. *SHELXTL*, Vol. V, Siemens Analytical X-ray Instrument Inc., Madison, WI, USA (1998).
[15] L. Gutierrez, G. Alzuet, J.A. Real, J. Cano, J. Borrás, A. Castiñeiras. *Inorg. Chem.*, **39**, 3608 (2000).
[16] G. Christou, JaS.P. Perlepes, E. Libby, K. Folting, J.C. Huffman, R.J. Webb, D.N. Hendrickson. *Inorg. Chem.*, **29**, 3657 (1990).
[17] H.-J. Chen, J. Zhang, W.-L. Feng, M. Fu. *Inorg. Chem. Commun.*, **9**, 300 (2006).
[18] S. Durot, C. Policar, G. Pelosi, F. Bisceglie, T. Mallah, J.-P. Mahy. *Inorg. Chem.*, **42**, 8072 (2003).
[19] C.S. Hong, Y.K. Do. *Inorg. Chem.*, **37**, 4470 (1998).
[20] W. Hiller, J. Straehle, A. Datz, M. Hanack, W.E. Hatfield, L.W. Ter Haar, P. Guetlich. *J. Am. Chem. Soc.*, **106**, 329 (1984).
[21] C.J. O'Conner. *Prog. Inorg. Chem.*, **29**, 203 (1982).
[22] M.E. Fisher. *Am. J. Phys.*, **32**, 343 (1964).
[23] O. Kahn. *Molecular Magnetism*, VCH, New York (1993).
[24] S.G. Baca, I.G. Filippova, O.A. Gherco, M. Gdaniec, Y.A. Simonov, N.V. Gerbeleu, P. Franz, R. Basler, S. Decurtins. *Inorg. Chim. Acta*, **357**, 3419 (2004).
[25] W. Han, L. Li, W. Gu, Z.-Q. Liu, S.-P. Yan, D.-Z. Liao, Z.-H. Jiang, P.-W. Shen. *Inorg. Chem. Commun.*, **7**, 228 (2004).
[26] W. Zhao, Y. Song, T.-A. Okamura, J. Fan, W.-Y. Sun, N. Ueyama. *Inorg. Chem.*, **44**(9), 3330 (2005).